Theory of doubly resonant infrared-visible sum-frequency and difference-frequency generation from adsorbed molecules

Jung Y. Huang
Institute of Electro-Optical Engineering, Chiao Tung University, Hsinchu, Taiwan, Republic of China

Y. R. Shen
Department of Physics, University of California at Berkeley, Berkeley, California 94720
and Materials Sciences Division, Lawrence Berkeley Laboratory, Berkeley, California 94720
(Received 20 December 1993)

We theoretically analyze doubly resonant infrared-visible sum-frequency (DR IVSFG) and difference-frequency generation (DR IVDFG) from a monolayer of adsorbates at an interface. Our calculated results with a model molecule indicate that the resonant amplitude of nonlinear optical susceptibility of DR IVDFG and DR IVSFG processes conveys information about the electron-vibration coupling in adsorbates. Moreover, owing to a dephasing-rephasing procedure involved, DR IVDFG can also be developed into a sensitive probe for investigating the coherent phase relaxation process in adsorbed molecules without the complication of inhomogeneous broadening.

PACS number(s): 42.50.Md, 68.35.Ja

I. INTRODUCTION

Molecules at an interface often behave differently than they do in bulk. This may be ascribed to the fact that molecules at surfaces are better oriented [1] and their electronic structures are modified by the interaction with substrate [2]. Therefore probing the orientation and electronic structures of molecules at an interface becomes an essential step for better understanding of the surface dynamics and chemistry of adsorbates.

Recently, second-order nonlinear optical effects have been demonstrated to be an effective and versatile probe of the static [3,4] and dynamic [5,6] properties of molecules and surfaces. During this investigation, various mechanisms of resonance enhancement were used to improve the spectroscopic capability of these techniques. In fact, fairly good agreement between the theoretical calculation and experimental result of resonant second-harmonic generation (SHG) from molecular systems has been achieved [7]. Unfortunately, the line shape of resonant SHG is often too broad to be sensitive enough for identifying molecular species. This, however, has been shown to be remedied by a newly developed technique called infrared-visible sum-frequency generation (IVSFG) [3].

IVSFG is also a second-order nonlinear optical process in which two input laser beams, one at the infrared frequency ω_1 and the other at the visible frequency ω_2, interact and generate an output at the sum-frequency $\omega_s=\omega_1+\omega_2$ in the visible spectrum of light. The IVSFG signal from an interface can be resonantly enhanced if ω_1 approaches a surface vibrational resonance. The enhanced IVSFG signal thus carries the vibrational spectroscopic information about the interface. It is noted that the signal strength of IVSFG can be further increased by an electronic resonance when either the input visible frequency (ω_2) or output sum frequency is near an electronic transition. Because the electronic and vibrational transitions are excited simultaneously in this doubly resonant process, IVSFG near double resonance is ideal for investigating electron-vibration coupling in adsorbates. Such a coupling is known to play an important role in the coherent evolution of a vibrational wave packet in an electronic state.

The ability to probe the coherent evolution of a surface excitation is crucial for understanding the dynamics and surface reaction of adsorbed molecules [8]. In the past, this was conducted by probing the phase relaxation processes through the measurement of the excitational linewidth [9]. Theoretical effort to understand such surface relaxation is then focused on relaxation models that can produce the measured spectral line shape [10]. However, the width of a spectral line is often dominated by inhomogeneous broadening. To find the homogeneous linewidth, i.e, the inverse of the dephasing time, it is necessary to resort to spectroscopic techniques capable of suppressing inhomogeneous broadening [11] or directly measure the phase relaxation rate in time domain with coherent optical processes such as photon echoes [12].

A one-to-one correspondence between each wave-mixing process capable of producing spectra with reduced inhomogeneous broadening and photon-echo processes was established [13]. In a recent study, Shen further pointed out that doubly resonant difference-frequency generation (DR DFG) in the time domain with properly time-ordered input pulses can yield an output in the form of a rephased echo [14]. This immediately suggests that doubly resonant infrared-visible difference-frequency generation (DR IVDFG) be used to probe the coherent phase relaxation of surface vibrations without resorting to higher-order nonlinear optical processes [25]. In this paper, we consider this aspect of DR IVDFG and its use as the probe of the coupling between electronic state and vibrational modes of adsorbed molecules at surfaces.

II. THEORY

A. Doubly resonant infrared-visible sum-frequency generation

The general theory of sum-frequency generation (SFG) in reflection from the surface of a nonlinear medium has been described in detail elsewhere [15]. As shown in Fig. 1, we explore surface SFG in reflection (K_s) from an interface between linear media 1 and 2 with a dielectric constant of ε_1 and ε_2, respectively.

We consider the case in which the visible frequency (ω_2) in the SFG process is close to a vibronic transition from the ground electronic state manifold $S_0\{gb\}$ to the first excited state $S_1\{ev\}$ and ω_1 in resonance with ω_{ba} [see Fig. 2(a)]. By applying the diagrammatic technique of Yee and Gustafson [13,16] to Fig. 2(b), the doubly resonant nonlinear polarizability can be expressed as

$$\alpha^{(2)}_{s,ijk}(-\omega_s;\omega_2,\omega_1)=\frac{-e^3}{\hbar^2}\sum_a \rho^{(0)}_{aa}\sum_b \frac{\langle gb|r_k|ga\rangle}{(\omega_1-\omega_{gbga}+i\gamma_{ba})}\sum_\nu \frac{\langle ga|r_i|ev\rangle\langle ev|r_j|gb\rangle}{(\omega_s-\omega_{evga}+i\gamma_{eg})} . \quad (1)$$

Here $\omega_{evga}=(E_{ev}-E_{ga})/\hbar$ is the frequency of the transition $|ev\rangle\leftarrow|ga\rangle$. A common Lorentzian linewidth is taken for each Franck-Condon (FC) transition (i.e., $\gamma_{evga}=\gamma_{eg}$). The above equation is conveniently rewritten by introducing the integral representation of energy denominators: $(a+ib)^{-1}=(-i)\int_0^\infty e^{it(a+ib)}dt$ for $b>0$ [17]. After applying the closure property of the vibrational manifolds, Eq. (1) becomes

$$\alpha^{(2)}_{s,ijk}(-\omega_s;\omega_2,\omega_1)=\frac{e^3}{\hbar^2}\int_0^\infty e^{i\omega_s t-\gamma_{eg}t+i\omega_1 t'-\gamma_{ba}t'}\langle\langle e^{itH_g(q)/\hbar}r_i^{ge}(q)e^{-itH_e(q)/\hbar}r_j^{eg}(q)e^{-it'H_g(q)/\hbar}r_k^{gg}(q)e^{it'H_g(q)/\hbar}\rangle\rangle dt\,dt' . \quad (2)$$

Here, $H_g(q)$ and $H_e(q)$ are the vibrational Hamiltonians of molecules in the electronic ground and excited states. $-er_i^{ge}(q)$ denotes the ith component of the electronic transition moment from the ground to excited state, and $-er_k^{gg}(q)$ denotes the kth component of the electric dipole moment of the ground state. The double bracket indicates the thermal average of the operators involved.

The $3N-6$ normal modes of a polyatomic molecule can be separated into two groups: The first group is comprised of the totally symmetric normal modes that are strongly Franck-Condon active in an optical transition; and the second is formed by the partially symmetric normal modes that are either FC inactive or weakly active in the optical transition. For a totally symmetric vibration, the excited-state potentials can be displaced in the equilibrium configuration relative to the ground-state surface. The displaced excited-state surface exerts a net force on the initially prepared wave packet, causing its mean position to move, hence the dynamic process of the wave packet is an important factor in the resonant excitation of a totally symmetric vibration.

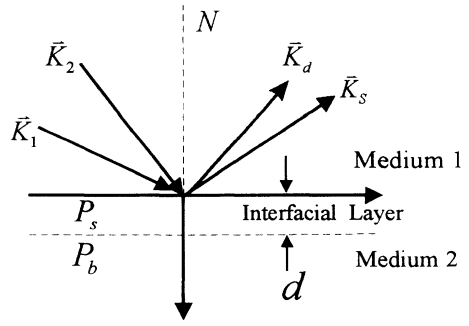

FIG. 1. Geometry of sum-frequency (K_s) and difference-frequency (K_d) generation from an interface in the reflected direction. The z direction is taken as zero at the interface between the media and is positive going into medium 2.

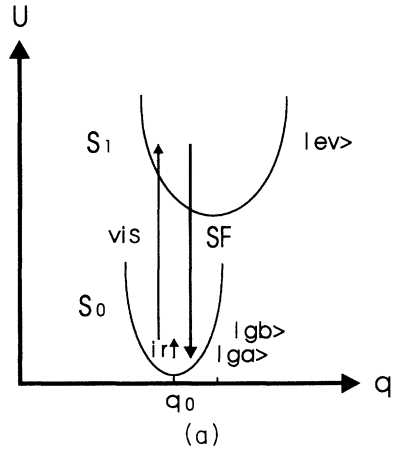

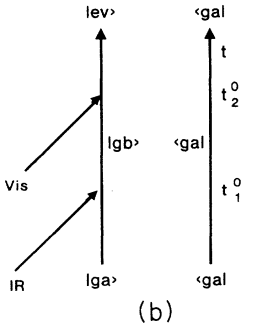

FIG. 2. (a) Schematic for doubly resonant infrared-visible sum-frequency generation process between the potential energy surfaces of the electronic ground state $\{S_0\}$ and the first electronic excited state $\{S_1\}$, and (b) the corresponding double Feynman diagram.

The random perturbation of the partially symmetric normal modes on the periodic motion of an optically active vibration is embedded in the radiative damping constant of the FC active vibration [18]. Similarly to the case observed with resonance Raman scattering (RRS) [17,19], the electron-vibration coupling in each optically active mode will also contribute to DR IVSFG. In the approximation of the Born-Oppenheimer separation of electronic and nuclear motions, a single-photon allowed vibronic transition is found to be described very well by a linearly coupled vibronic system. The linearly displaced vibrational Hamiltonian of the excited state in this model has the form [19]

$$H_e(q)=H_g(q)+i\sum_f L_f(a_f-a_f^\dagger)+\hbar\omega_{eg} \ . \tag{3}$$

Here, L_f denotes the linear electron-phonon coupling coefficient, $\hbar\omega_{eg}$ is the electronic transition energy appropriate to the ground electronic state equilibrium configuration ($q=0$), and a_f and $a_f^\dagger$ are phonon annihilation and creation operators. We also have $H_g(q)=\sum_f \hbar\omega_f(a_f^\dagger a_f+\frac{1}{2})$.

Equation (3) can be conveniently converted to the following form [19]:

$$H_e(q)=e^P H_g(q)e^{-P}+\hbar\omega_{eg}^0 \ , \tag{4}$$

where $P=i\sum_f \xi_f(a_f+a_f^\dagger)$, with $\xi_f=L_f/(\hbar\omega_f)$. The quantity $\omega_{eg}^0=\omega_{eg}-\sum_f \xi_f^2\omega_f$ is the zero-phonon transition frequency. The electronic transition moment function $-er^{eg}(q)$ for a totally symmetric normal mode can be replaced by a constant which is the value evaluated at the equilibrium configuration ($q=0$) of the ground electronic state, i.e., the Condon approximation

$$-er^{eg}(q)\cong -er^{eg}(q=0) \ . \tag{5a}$$

This is a good approximation for strongly FC active modes that are known to be significantly affected by the dynamics of wave packets. Vibronic coupling between two excited electronic states can lead to linear terms in the expansion of $-er^{eg}(q)$. However, this does not become a restriction in our molecular model of DR IVSFG because linear non-Condon terms can be included without much difficulty in calculating Eq. (2) [19]. The ground-state dipole moment of a molecule resonantly excited by an infrared photon, however, is modulated by the vibrations of the molecule:

$$\begin{aligned} r^{gg}(q)&\cong r^{gg}(0)+\sum_f \frac{\partial r^{gg}}{\partial q_f}q_f \\ &=r^{gg}(0)+i\sum_f \frac{\partial r^{gg}}{\partial q_f}(a_f-a_f^\dagger) \\ &=r^{gg}(0)[1+D_g] \ . \end{aligned} \tag{5b}$$

Substituting Eqs. (4) and (5) into Eq. (2), we obtain

$$\begin{aligned} &\alpha_{s,ijk}^{(2)}(-\omega_s;\omega_2,\omega_1)=\frac{e^3}{\hbar^2}r_i^{eg}(0)r_j^{ge}(0)r_k^{gg}(0)\int_0^\infty e^{i\omega_s t-\gamma_{eg}t+i\omega_1 t'-\gamma_f t'}f(t,t')dt\,dt' \ , \\ &f(t,t')=\langle\langle e^{itH_g/\hbar}e^P e^{-itH_g/\hbar}e^{-P}e^{-it'H_g/\hbar}(1+D_g)e^{it'H_g/\hbar}\rangle\rangle \\ &\quad=\langle\langle e^{P(t)}e^{-P}[1+D_g(-t')]\rangle\rangle \ . \end{aligned} \tag{6}$$

To evaluate $f(t,t')$, the function $f(\Lambda;t,t')=\langle\langle e^{P(t)}e^{-P}e^{\Lambda D_g(-t')}\rangle\rangle$ is defined and then reduced to a product of c numbers through the use of boson algebra identities [19,20]. If we expand $\exp[\Lambda D_g(-t')]$ to a term linear in Λ, we can then set $\Lambda=1$ to recover the thermal average $f(t,t')$. Thus $\alpha_{s,ijk}^{(2)}$ in finite temperatures can be found to have the expression

$$\alpha_{s,ijk}^{(2)}(-\omega_s;\omega_2,\omega_1)=\sum_f \frac{S_{f,ijk}}{(\omega_1-\omega_f)+i\gamma_f} \ , \tag{7}$$

$$\begin{aligned} S_{f,ijk}&=\frac{e^3}{\hbar^2}\xi_f r_i^{ge}(0)r_j^{eg}(0)\Delta r_k^{gg}(0) \\ &\quad\times[(\bar{n}_f+1)\Phi(\omega_s-\omega_f)-\Phi(\omega_s)] \ , \end{aligned}$$

where $\bar{n}_f=1/[\exp(\hbar\omega_f/k_BT)-1]$, and $\Delta r_k^{gg}(0)\equiv[dr_k^{gg}(q)/dq]_{q=0}$ is the ground-state dipole moment derivative. $\Phi(\omega)$ is the Fourier transform of the overlap function of the time-evolved wave packet [21]

$$\begin{aligned} &\Phi(\omega)=i\int_0^\infty\langle a|a(t)\rangle e^{i(\omega-\omega_{eg}^0)t-\gamma_{eg}t}dt \ , \\ &\langle a|a(t)\rangle=\exp\left[\sum_f \xi_f^2[(\bar{n}_f+1)(e^{-i\omega_f t}-1)\right. \\ &\qquad\left.+\bar{n}_f(e^{i\omega_f t}-1)]\right] \ . \end{aligned} \tag{8}$$

Here $|a(t)\rangle=\exp[iH_e(q)t]|a\rangle$ describes the evolution of the vibrational wave packet in the excited electronic state, initially prepared by an optical transition from the ground state $|ga\rangle$. The single-photon absorption spectrum of a molecule, $\sigma(\omega)/\omega$, is equal to the imaginary part of $\Phi(\omega)$ by [17]

$$\begin{aligned} \frac{\sigma(\omega)}{\omega}&=\int_{-\infty}^\infty\langle a|a(t)\rangle e^{i(\omega-\omega_{eg}^0)t-\gamma_{eg}|t|}dt \\ &=\mathrm{Im}[\Phi(\omega-\omega_{eg}^0)] \ . \end{aligned} \tag{9}$$

Note that all the information about molecular electronic structure has been absorbed into the time evolution behavior of the wave packet. This formalism of DR IVSFG allows us to skip the difficulty of the sum-over-

states approach and focus on key physical parameters.

Equations (7)–(9) provide a connection between the absorption spectrum and the SFG excitation profiles (S_f vs ω_2) of normal modes of adsorbates. $[(\bar{n}_f+1)\Phi(\omega_s-\omega_f)-\Phi(\omega_s)]$, which appears in the resonant amplitude of DR IVSFG, is similar to that found in the time-correlator formulation of resonance Raman scattering [18]. In Eq. (7), $\{\xi_f, \omega_f, \gamma_f, \gamma_{eg}$, and $\omega_{eg}^0\}$ are used to describe DR IVSFG. These parameters are also indispensable for elucidating the dynamical properties of molecules. We will show that these parameters can be determined from the fit of the experimental DR IVSFG excitation profiles to Eq. (7) in the discussion section.

B. Doubly resonant infrared-visible difference-frequency generation

In addition to the SFG beam, a difference-frequency signal (K_d) also emerges from the interface, as shown in Fig. 1. The doubly resonant difference-frequency generation is especially interesting since it can suppress inhomogeneous broadening, as pointed out by Shen [14]. To further reveal its potential applications, we analyze the case in which the visible frequency in the DR IVDFG process is close to a transition from the electronic ground-state manifold $S_0\{ga\}$ to the first excited state $S_1\{ev\}$ [see Fig. 3(a)]. The resonant nonlinear polarizability, $\alpha^{(2)}_{d,ijk}$, corresponding to Fig. 3(b) can be written as

$$\alpha^{(2)}_{d,ijk}(-\omega_d;\omega_2,\omega_1)=\frac{-e^3}{\hbar^2}\sum_a \rho^{(0)}_{aa}\sum_b\sum_\nu \frac{\langle gb|r_i|ev\rangle}{(\omega_1-\omega_{gbga}-i\gamma_{ba})}\frac{\langle ev|r_j|ga\rangle\langle ga|r_k|gb\rangle}{[(\omega_2-\omega_1)-\omega_{evgb}+i\gamma_{eg}]} . \tag{10}$$

Following the same procedure as detailed in Sec. II A, we can readily obtain

$$\alpha^{(2)}_{d,ijk}(-\omega_d;\omega_2,\omega_1)=\sum_f \frac{D_{f,ijk}}{(\omega_1-\omega_f)-i\gamma_f} ,$$
$$D_{f,ijk}=\frac{e^3}{\hbar^2}\xi_f r_i^{ge}(0)r_j^{eg}(0)\Delta r_k^{gg}(0) \times[\Phi(\omega_d+\omega_f)-\Phi(\omega_d)](\bar{n}_f+1) . \tag{11}$$

Note that at zero temperature the intensity profile of first-order Raman scattering from the fth vibrational mode, $I_f(\omega_2)$, is proportional to $|\Phi(\omega_2)-\Phi(\omega_2-\omega_f)|^2$, which is essentially the same as the absolute square of $D_{f,ijk}$ of Eq. (11). Thus the excitation profiles of DR IVDFG carry dynamical information about wave packets which is similar to what is widely recognized in resonance Raman scattering.

C. Inhomogeneous broadening

The resonant frequencies of a molecular system often depend on its local environment. To account for this possible inhomogeneous broadening, the nonlinear susceptibility should be convolved with a Gaussian distribution function of the resonant frequencies, giving

$$\chi^{(2)}_d(\omega_d=\omega_2-\omega_1)=N\int \frac{1}{\sqrt{\pi}\eta_0}e^{-(\eta/\eta_0)^2}[\alpha^{(2)}_d(\omega_d,\eta)]d\eta , \tag{12}$$

where η represents a set of local parameters. The resonant frequencies of adsorbates in different local environments can be expressed as [22]

$$\omega_{eg}=\Omega_{eg}+\Delta\omega_{eg}(\eta)=\Omega_{eg}+\eta\Delta\omega_{eg} ,$$
$$\omega_f=\omega_f^0+\Delta\omega_f(\eta)=\omega_f^0+\eta\Delta\omega_f , \tag{13}$$

assuming a single dominant inhomogeneous broadening channel. By substituting Eq. (8) into Eq. (11), we can rewrite the nonlinear susceptibility of DR IVDFG as

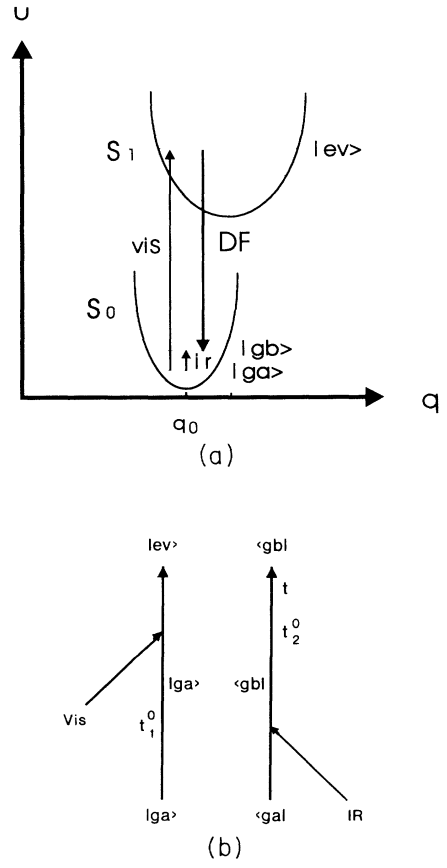

FIG. 3. Schematic for (a) the energy level and (b) the corresponding double Feynman diagram of doubly resonant infrared-visible difference-frequency generation process.

$$\chi^{(2)}_{d,ijk}(-\omega_d;\omega_1,\omega_2)=-\frac{Ne^3}{\hbar^2}\sum_f \xi_f r_i^{ge} r_j^{eg}\Delta r_k^{gg} \times \sum_{n_1=0}^{\infty}\cdots\sum_{n_N=0}^{\infty}\left[\prod_{Q=1}^{N}\frac{\xi_Q^{2n_Q}e^{-\xi_Q^2}}{n_Q!}\right]\int_{-\infty}^{+\infty}\frac{1}{\sqrt{\pi}\eta_0}e^{-(\eta/\eta_0)^2}\frac{d\eta}{(\omega_1-\omega_f^0-\eta\Delta\omega_f-i\gamma_f)} \times\left[\frac{1}{[\omega_2-\omega_1+(\omega_f^0+\eta\Delta\omega_f)-(\eta\Delta\omega_{eg}+\Omega_{eg})-\sum_{Q=1}^{N}n_Q(\omega_Q^0+\eta\Delta\omega_Q)+i\gamma_{eg}]}-\frac{1}{[\omega_2-\omega_1-(\eta\Delta\omega_{eg}+\Omega_{eg})-\sum_{Q=1}^{N}n_Q(\omega_Q^0+\eta\Delta\omega_Q)+i\gamma_{eg}]}\right]. \tag{14}$$

By using the properties of the plasma dispersion function, Oudar and Shen [22] have shown that in a double-resonance case, if the imaginary parts of the energy denominators in nonlinear optical susceptibility (χ) have opposite signs, then χ scanned over the resonance yields a spectral line with a Lorentzian linewidth. Indeed, near the double resonance (i.e., $\omega_1=\omega_f^0$ and $\omega_d=-\omega_f^0+\Omega_{eg}+\sum_Q n_Q\omega_Q^0$ or $\omega_1=\omega_f^0$ and $\omega_d=\Omega_{eg}+\sum_Q n_Q\omega_Q^0$) Eq. (14) exhibits a Lorentzian line shape with a half-width of $\gamma_f+\gamma_{eg}$. On the contrary, this is not the case for DR IVSFG where the imaginary parts of the denominators in $\chi_s^{(2)}$ have the same sign. Thus $\chi_s^{(2)}$ exhibits no singularity near the double resonance. In fact, at the double resonance, $\chi_s^{(2)}(-\omega_s;\omega_1,\omega_2)$ exhibits a width more than twice the width of inhomogeneous broadening.

D. Transient effect

The reduced spectral linewidth via DR IVDFG can be better appreciated in the time domain. The coherence between $|ev\rangle$ and $\langle gb|$ [see Fig. 3(b)], which is set up by $E(\omega_1)$ and $E(\omega_2)$, can directly emit the output radiation at $\omega_d=\omega_2-\omega_1$ if transition between $|ev\rangle$ and $\langle gb|$ is single-photon allowed. The polarization set up by pulsed excitations has different phases for different molecules in different local environments. The resulting dephased polarization can be expressed as

$$P_d^{(2)}(\omega_d=\omega_2-\omega_1,t)=N\int n(\eta)\mathrm{Tr}[-e\mathbf{r}\rho_d^{(2)}(t,\eta)]d\eta =(-e)N\left[\int n(\eta)\sum_b\sum_v\langle gb|r|ev\rangle\rho^{(2)}_{d,evgb}(t,\eta)d\eta+\text{c.c.}\right], \tag{15}$$

where $n(\eta)$ is the distribution function of inhomogeneous broadening and N the surface density. By following the diagrammatic rules of the time-dependent density matrix, we can write

$$\rho^{(2)}_{d,evgb}(t,\eta)=\frac{e^2}{\hbar^2}e^{i(\mathbf{k}_2-\mathbf{k}_1)\cdot\mathbf{r}(t)-i[\Omega_{eg}+(v-1)\omega_f^0]t-\gamma_{eg}t+\gamma_{eg}t_2^0-\gamma_f(t_2^0-t_1^0)} \times\sum_a\rho_{aa}^{(0)}\langle ev|r|ga\rangle\langle ga|r|gb\rangle\int_{-\infty}^{t}e^{i[(\Omega_{eg}-\omega_2+v\omega_f^0)t_2]}A_2(t_2)dt_2\int_{-\infty}^{t_2}e^{-i[\omega_f^0-\omega_1]t_1}A_1^*(t_1)dt_1e^{-i\theta_d(t,\eta)}, \tag{16}$$

assuming that each level in the vibrational manifolds of the excited and ground electronic states is equally affected by the inhomogeneous broadening. Here $\theta_d(t,\eta)=\{\Delta\omega_{eg}(\eta)t-[\Delta\omega_{eg}(\eta)t_2^0+\Delta\omega_{ba}(\eta)(t_2^0-t_1^0)]\}$ denotes the phase difference of the induced nonlinear polarization at the local environment specified by η; and $A_i(t_i)$ is the envelope of the exciting pulsed field which has a carrier frequency at ω_i and peaks at t_i^0. As noted from Eq. (16), all the molecules at the surface will generate the maximum coherent output whenever the phase difference vanishes [13,14], i.e., $\theta_d(t,\eta)=0$,

$$t_e=t_2^0+\frac{\Delta\omega_{ba}(\eta)}{\Delta\omega_{eg}(\eta)}(t_2^0-t_1^0). \tag{17}$$

This indicates that with properly time-ordered input pulses ($t_2^0>t_1^0$), the transient DR IVDFG will give rise to a photon echo of frequency ω_d at $t=t_e$ which is later than both t_2^0 and t_1^0 [14] [see Fig. 4(a)]. The amplitude of the DR IVDFG echo pulse decays as $\exp[-\gamma_{eg}(t_e-t_2^0)-\gamma_f(t_2^0-t_1^0)]$ with the decay rate free from the influence of the inho-

mogeneous broadening. Thus in frequency domain DR IVDFG exhibits a reduced linewidth which contains the intrinsic dynamical information about molecules.

By applying similar analysis to DR IVSFG, we find

$$\rho^{(2)}_{s,evga}(t,\eta)=-\frac{e^2}{\hbar^2}e^{i(\mathbf{k}_2+\mathbf{k}_1)\cdot\mathbf{r}(t)-i(\Omega_{eg}+v\omega_f^0)t-\gamma_{eg}t+\gamma_{eg}t_2^0-\gamma_f(t_2^0-t_1^0)}$$
$$\times\sum_a\rho^{(0)}_{aa}\langle ev|r|gb\rangle\langle gb|r|ga\rangle\int_{-\infty}^{t}e^{i\{[\Omega_{eg}-\omega_2+(v-1)\omega_f^0]\}t_2}A_2(t_1)dt_2\int_{-\infty}^{t_2}e^{i[\omega_f^0-\omega_1]t_1}A_1(t_1)dt_1e^{-i\theta_s(t,\eta)}, \quad (18)$$

where $\theta_s(t,\eta)=\{\Delta\omega_{eg}(\eta)t-[\Delta\omega_{eg}(\eta)t_2^0-\Delta\omega_{ba}(\eta)(t_2^0-t_1^0)]\}$. The time at which $\theta_s=0$ is always less than t_2^0 [see Fig. 4(b)]. Therefore DR IVSFG does not involve a dephasing-rephasing process of photon echoes and its spectral line will be affected by inhomogeneous broadening.

III. NUMERICAL RESULTS AND DISCUSSION

The chemisorption of molecules on a substrate not only can perturb the electronic states of the substrate but also change the potential energy surfaces and vibrational structures of adsorbates [2]. These changes, once they have been measured, could yield valuable information about the static and dynamical behaviors of adsorbates. In this section, we will show that such measurements can be fulfilled effectively by the use of DR IVSFG and DR IVDF G processes.

It is noted that Eqs. (7) and (9) allow the connection between the absorption spectrum and DR IVSFG amplitudes of normal modes of adsorbates. This relation is similar to the transform theory of resonance Raman scattering [17], which seeks to determine the Raman excitation profile (REP) from the absorption cross section. In an indirect approach of RRS model potentials are used to calculate the time cross correlation function ($\langle b|a(t)\rangle$) which can then be transformed to the frequency domain. The parameters of the potential energy surfaces can be adjusted in order to get a good fit of the experimental profile. In this respect, a direct inversion of resonant Raman excitation profiles to yield time domain information is more attractive. Recently, a direct inversion scheme has been proven to be feasible [23].

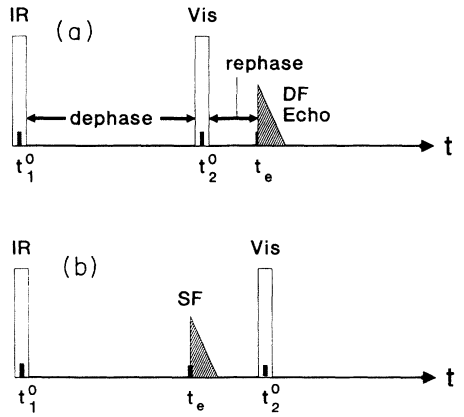

FIG. 4. Pulse sequences for (a) transient infrared-visible difference-frequency generation, and (b) sum-frequency generation processes.

In the case of an interfacial system, DR IVSFG and DR IVDFG can be used to determine the parameters of the vibrational structures and potential energy surfaces of adsorbed molecules, which are indicated by $\{\xi_f, \omega_f, \gamma_f, \gamma_{eg}, \omega_{eg}^0$, and $\eta_0\Delta\omega_{eg}\}$. From the experimental point of view, this approach can be done by first scanning the infrared beam (ω_1) through each vibrational mode with a fixed visible frequency. Equation (7) is then used to fit the observed resonant nonlinear optical susceptibility. The fit determines ω_f, γ_f, and S_f. In the second step, we let $\omega_1=\omega_f$ and measure S_f as a function of ω_2. This measurement yields a set of excitation profiles of DR IVSFG. In an indirect approach, we can fit these DR IVSFG profiles to Eq. (7) with the help of model potential surfaces to determine the rest parameters (ξ_f, γ_{eg}, $\eta_0\Delta\omega_{eg}$, and ω_{eg}^0). We will elucidate this procedure in detail by using a model molecule with linearly displaced harmonic potential surfaces along three FC active normal mode coordinates. The vibrational frequencies and displacement parameters of these vibrational modes are described in Table I.

Figure 5 shows the calculated absorption spectra of the model molecule, for which the short-dashed, solid, and dotted curves are the calculated results obtained with the displacement parameters $\{\xi_f\}$ taken from sets 1, 2, and 3, respectively. In the calculations, we model the homogeneous broadening of an electronic transition by a damping constant, γ_{eg}, and the inhomogeneous broadening by the parameter of $\eta\Delta\omega_{eg}$ [see Eq. (13)]. In Fig. 5, these two parameters are assumed to be (a) $\gamma_{eg}=300$ cm^{-1}, $\eta\Delta\omega_{eg}=0$ cm^{-1}; (b) $\gamma_{eg}=600$ cm^{-1}, $\eta\Delta\omega_{eg}=0$ cm^{-1}; and (c) $\gamma_{eg}=300$ cm^{-1}, $\eta\Delta\omega_{eg}=300$ cm^{-1}. As expected, the higher vibronic features in the absorption spectra become more distinctive when the linear electron-phonon coupling is increased ($\xi_3=0.7$: short-

TABLE I. The frequencies, ω_f, and displacement parameters, ξ_f, of three Franck-Condon active vibrational normal modes of a model molecule.

		ξ_f		
Mode no.	ω_f (cm^{-1})	Set 1	Set 2	Set 3
1	900	0.3	0.3	0.3
2	1200	0.6	0.6	0.6
3	1500	0.7	1.0	1.5

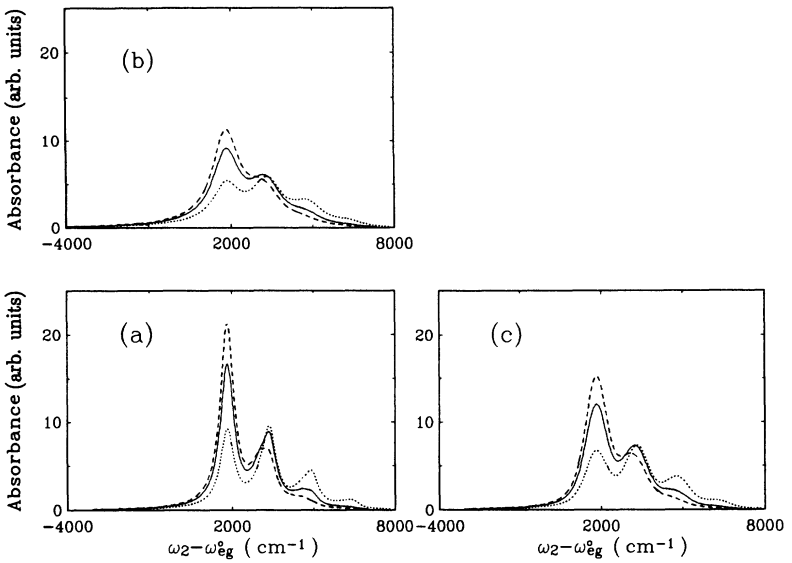

FIG. 5. Calculated absorption spectra for linearly displaced harmonic potential energy surfaces along Franck-Condon active normal mode coordinates. The vibrational frequencies and displacement parameters of this model molecule are described in Table I. The calculated spectrum with the displacement parameters, $\{\xi_f\}$, taken from set 1 in Table I is indicated by the short-dashed curve; solid curve is from set 2, and dotted curve for set 3. In addition, the electronic damping constant γ_{eg} and inhomogeneous broadening parameter $\eta_0\Delta\omega_{eg}$ are assumed to be (a) $\gamma_{eg}=300$ cm^{-1}, $\eta_0\Delta\omega_{eg}=0$ cm^{-1}; (b) $\gamma_{eg}=600$ cm^{-1}, $\eta_0\Delta\omega_{eg}=0$ cm^{-1}; and (c) $\gamma_{eg}=300$ cm^{-1}, $\eta_0\Delta\omega_{eg}=300$ cm^{-1}.

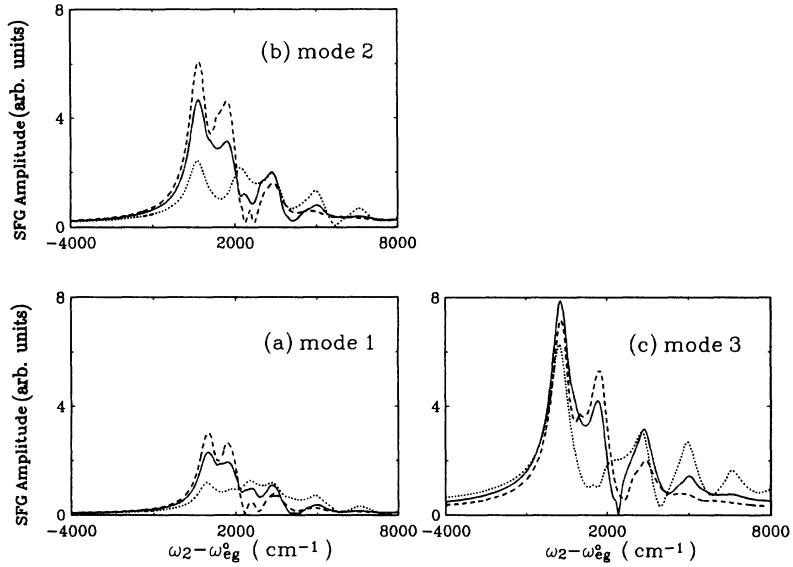

FIG. 6. The resonant amplitude, $S_f(-\omega_2-\omega_f;\omega_2,\omega_f)$, of DR IVSFG for each vibrational normal mode is plotted as a function of the visible frequency $(\omega_2-\omega^0_{eg})$. The absorption spectra of the molecule are shown in Fig. 5(a).

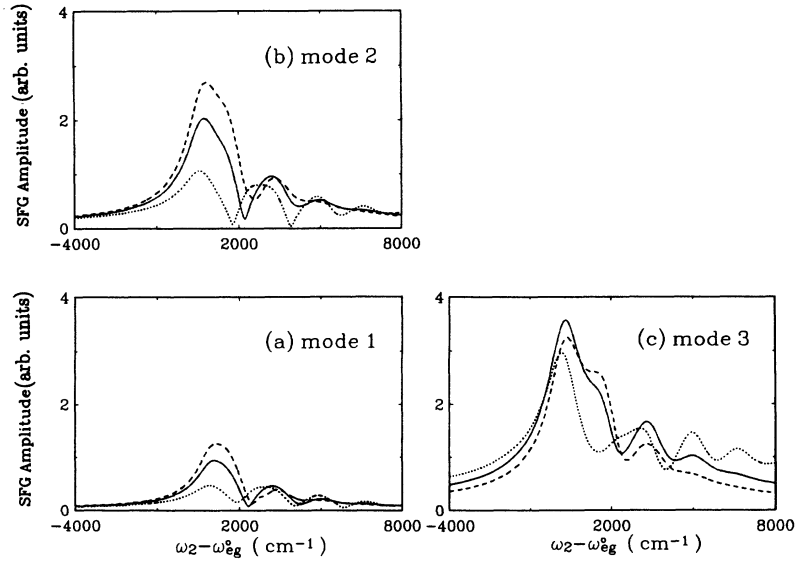

FIG. 7. The resonant amplitude $S_f(-\omega_2-\omega_f;\omega_2,\omega_f)$ of DR IVSFG for each vibrational normal mode is plotted as a function of the visible frequency $(\omega_2-\omega^0_{eg})$. The absorption spectra of the molecule are shown in Fig. 5(b).

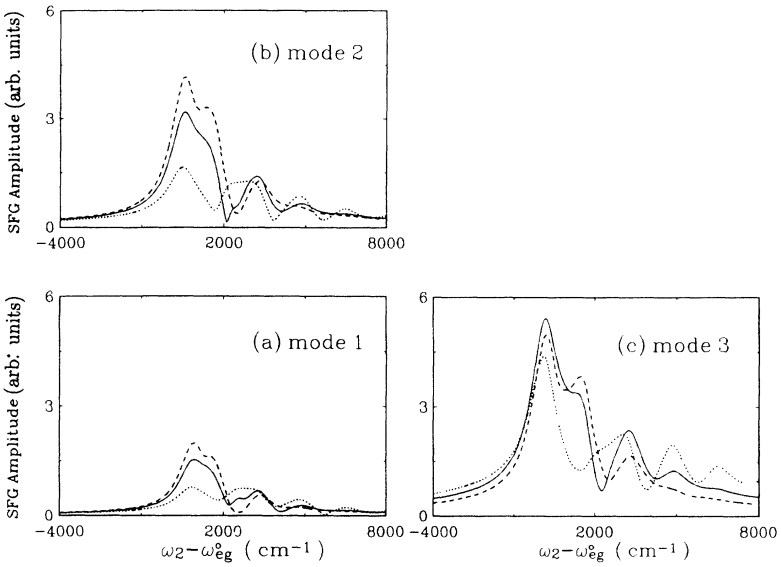

FIG. 8. The resonant amplitude S_f of DR IVSFG for each vibrational normal mode is plotted as a function of the visible frequency $(\omega_2-\omega_{eg}^0)$. The absorption spectra of the molecule are shown in Fig. 5(c).

dashed line; $\xi_3=1.0$: solid line; and $\xi_3=1.5$: dotted). By comparing Fig. 5(b) with 5(c), we note that the separation of the line broadening into the homogeneous and inhomogeneous parts leads to different absorption strength. But the difference in the absorption line shape between two cases cannot be detected clearly.

The displaced difference operation on Φ gives rise to the sensitive dependence of S_f on ξ_f. This can be clearly seen in Fig. 6, where the resonant amplitude $S_{f,ijk}(-\omega_2-\omega_f;\omega_2,\omega_f)$ of DR IVSFG for each vibrational normal mode is plotted as a function of the visible frequency $(\omega_2-\omega_{eg}^0)$. The corresponding molecular absorption spectra are depicted in Fig. 5(a). It is interesting to note that the position of the second peak ($\sim$1825 cm^{-1}) in Fig. 6 coincides with that of the first vibronic peak of the absorption spectra [see Fig. 5(a)]. Furthermore, the frequency difference of the first and second spectral peaks in Fig. 6 is identical to the corresponding normal mode frequency. In addition, ξ_3 not only changes the line shape (S_3) of mode 3 but also affects the profiles of the other two normal modes. Particularly noticeable, the second peak height of S_f is found to decrease as ξ_3 increases. At sufficiently large ξ_3, this peak disappears completely. The molecule with larger broadening exhibits a similar trend, which is depicted in Figs. 7 and 8. From the comparison between Figs. 7 and 8, we can find that S_f can resolve the effect of the homogeneous and inhomogeneous broadening with higher accuracy than that with absorption spectrum. Moreover, with the immunity of DR IVDFG to inhomogeneous broadening, we can in principle measure the homogeneous broadening directly from the spectral profiles of DR IVDFG. Even by using DR IVSFG only, a good fit of the excitation profiles provides a very strict test for the parameters used. The simulations show that S_f as a function of ω_2 indeed accurately reflects the electron-vibration coupling in an adsorbate.

Recently, the application of the resonant third-harmonic generation (THG) technique to investigate the vibronic structures of all-trans β-carotene in solution has been reported by van Beek, Kajzar, and Albrecht [24]. Their results indicate that a suitable fit of the nonlinear third-harmonic susceptibility dispersion could be accomplished using fewer FC active normal modes, but all FC active normal modes in an electronic transition are required to correctly fit the observed resonance Raman excitation profiles. The higher sensitivity of REP to the vibrational structures of molecules can be attributed to the selective excitation of molecular vibrations, which appears in RRS but not in THG. The resonant vibrational transitions induced by the infrared photons in DR IVSFG and DR IVDFG processes warranty the sensitivity to the vibronic structures of molecules. In addition, both DR IVSFG and DR IVDFG belong to a lower-order wave-mixing process with double-resonance enhancement, therefore they are capable of generating stronger signal than that via RRS and other higher-order wave-mixing processes [25,26]. Furthermore, DR IVDFG and DR IVSFG are surface specific, thus are ideally suited for surface studies.

In summary, an analytic expression of doubly resonant infrared-visible difference-frequency and sum-frequency susceptibilities in terms of the overlap function of the wave packet in an excited electronic state has been derived. Our results show that these second-order nonlinear optical effects can be developed into an effective probe for the electron-vibration coupling in molecules adsorbed at surfaces. In time domain, DR IVDFG is found to go through a dephasing-rephasing process of photon echoes, therefore it can become a sensitive technique for the investigation of coherent dynamical processes appearing at surfaces.

ACKNOWLEDGMENT

The author (J.Y.H.) acknowledges the financial support from the National Science Council of ROC under Grant No. NSC81-0208-M009-01.

[1] K. Bhattacharyya, A. Castro, E. V. Sitzmann, and K. B. Eisenthal, J. Chem. Phys. **89**, 3376 (1988).
[2] W. Brenig, S. Kuchenhoff, and H. Kasai, Appl. Phys. A **51**, 115 (1990).
[3] See, for example, Y. R. Shen, Nature (London) **337**, 519 (1989), and references therein.
[4] T. F. Heinz, C. K. Chen, D. Ricard, and Y. R. Shen, Phys. Rev. Lett. **48**, 478 (1982).
[5] P. Saeta, J.-K. Wang, Y. Siegal, N. Bloembergen, and E. Mazur, Phys. Rev. Lett. **67**, 1023 (1991); X. D. Ziao, X. D. Zhu, W. Daum, and Y. R. Shen, *ibid.* **66**, 2352 (1991).
[6] A. L. Harris, L. Rothberg, L. H. Dubois, N. J. Levinos, and L. Dahr, Phys. Rev. Lett. **64**, 2086 (1990); P. Guyot-Sionnest, *ibid.* **66**, 1489 (1991); **67**, 2323 (1991).
[7] S. H. Lin, R. G. Alden, A. A. Villaeys, and V. Pfumio, Phys. Rev. A **48**, 3137 (1993).
[8] G. A. Somorjai, *Chemistry in Two Dimensions: Surfaces* (Cornell University Press, Ithaca, 1981), p. 360; J. W. Gadzuk, Appl. Phys. A **51**, 108 (1990).
[9] B. N. J. Persson and M. Persson, Solid State Commun. **36**, 175 (1980); Surf. Sci. **97**, 609 (1980).
[10] J. W. Gadzuk and A. C. Luntz, Surf. Sci. **144**, 429 (1984).
[11] W. Demtroder, *Laser Spectroscopy* (Springer-Verlag, Berlin, 1981).
[12] N. A. Kurnit, I. D. Abella, and S. R. Hartmann, Phys. Rev. Lett. **13**, 567 (1964).
[13] P. X. Ye and Y. R. Shen, Phys. Rev. A **25**, 2083 (1982).
[14] Y. R. Shen, Phys. Rev. A **45**, 446 (1992).
[15] P. Guyot-Sionnest, W. Chen, and Y. R. Shen, Phys. Rev. B **33**, 8254 (1986); P. Guyot-Sionnest and Y. R. Shen, *ibid.* **35**, 4420 (1987); **38**, 7985 (1989), and references therein.
[16] T. K. Yee and T. K. Gustafson, Phys. Rev. A **18**, 1597 (1978).
[17] J. B. Page and D. L. Tonks, J. Chem. Phys. **75**, 5694 (1981).
[18] R. M. Shelby, C. B. Harris, and P. A. Cornelius, J. Chem. Phys. **70**, 34 (1979); B. S. Neporent and V. S. Yarunin, Zh. Eksp. Teor. Fiz. **99**, 447 (1991) [Sov. Phys. JETP **72**, 249 (1991)].
[19] C. K. Chan, J. Chem. Phys. **81**, 1614 (1984).
[20] W. H. Louisell, *Quantum Statistical Properties of Radiation* (Wiley, New York, 1973).
[21] Z. Deng and S. Mukamel, J. Chem. Phys. **85**, 1738 (1986).
[22] J.-L. Oudar and Y. R. Shen, Phys. Rev. A **22**, 1141 (1980).
[23] F. Remacle and R. D. Levine, J. Chem. Phys. **99**, 4908 (1993).
[24] J. B. van Beek, F. Kajzar, and A. C. Albrecht, J. Chem. Phys. **95**, 6400 (1991).
[25] X. D. Zhu and Y. R. Shen, Appl. Phys. B **50**, 535 (1990); P. Guyot-Sionnest, Phys. Rev. Lett. **67**, 2323 (1991).
[26] A. A. Markarov, Chem. Phys. Lett. **190**, 236 (1992).

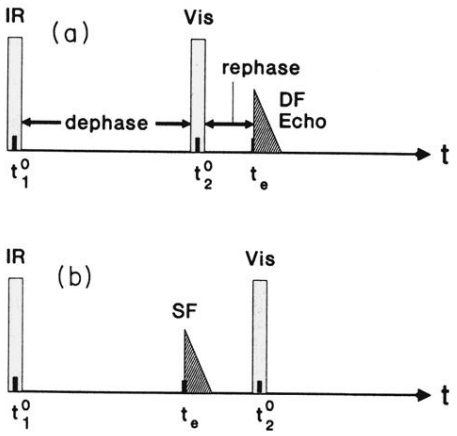

FIG. 4. Pulse sequences for (a) transient infrared-visible difference-frequency generation, and (b) sum-frequency generation processes.